Wake Tracking and the Detection of Vortex Rings by the Canal Lateral Line of Fish

Jan-Moritz P. Franosch,[1] Hendrik J. A. Hagedorn,[1] Julie Goulet,[1] Jacob Engelmann,[2] and J. Leo van Hemmen[1]

[1]*Physik Department T35, Technische Universität München, 85747 Garching bei München, Germany*

[2]*Institute of Zoology, Neuroethology—Sensory Ecology, Endenicher Allee 11-13, 53115 Bonn, Germany*

(Received 26 June 2008; published 13 August 2009)

Research on the lateral line of fish has mainly focused on the detection of oscillating objects. Yet many fish are able to track vortex wakes that arise from other fish. It is not yet known what the sensory input from a wake looks like and how fish can extract relevant information from it. We present a mathematical model to determine how vortices stimulate the canal lateral line and verify it by neuronal recordings. We also show how the information about the orientation of a vortex ring is captured by the lateral-line sensors so as to enable fish to follow a vortex street.

DOI: 10.1103/PhysRevLett.103.078102 PACS numbers: 87.19.ls, 47.32.ck, 87.19.lt

Fish measure the local water velocity and the pressure distribution through organs that are organized either in narrow tubes along or all over the body surface. This lateral-line system enables fish to localize and identify other moving objects [1–5]. Most lateral-line experiments have been done with oscillating spheres [2,6,7]. Then fish can extract relevant information from simple features of the resulting stimuli, such as maxima, minima, or zeros along the lateral line, and reconstruct the object's position and axis of oscillation [3,8,9].

It has become clear, however, that more natural stimuli need to be examined to further understand the lateral line's information processing. In general, fish generate wakes. The wake of a discontinuous swimmer consists of ring vortices originating from the beats and a trailing wake that compensates for the fish's displacement [10,11] (see Fig. 1). By conservation of angular momentum, ring vortices are stable in incompressible fluids with low viscosity ([12], Sec. 146), even under natural conditions [10,13]. The lateral drift of these rings is slow and tends to zero so that the wake structure only occupies a confined space [10]. Wake structures can thus serve as underwater traces and allow predators to detect their prey for a period of over a minute [14]. Catfish, for instance, simply track those wakes to locate their targets [15].

How, then, can fish perform wake tracking, what stimuli do they receive, and how can they exploit these stimuli? These are the questions we address, and solve, here.

The canal lateral line consists of an array of canals located alongside the fish body, directly underneath the skin, and connected to the outside through approximately equidistant pores. Between each two neighboring pores there is a cupula, a gelatinous body that covers hair-cell receptors protruding into the cupular base. These hair cells function as displacement detectors and produce neuronal action potentials in response to a displacement of their ciliary bundles. Local water motion deflects the cupulae. Since water motion in a canal is driven by the pressure difference between neighboring pores, the canal lateral-line system essentially monitors the spatial distribution of the pressure gradients alongside the fish body [16].

The alternating component of the spatial pressure gradient distribution is represented directly by the excitation patterns of the lateral-line nerves [1,9,17] and is therefore relevant information passed on to higher centers of the nervous system. The excitation patterns are influenced by the propulsive motion of the fish itself, but the fish is able to compensate for the resulting lateral-line signal, as shown by calculating pressure signals [18].

Artificially generated vortex rings that pass a fish laterally [19] as well as vortex rings that are part of a von Kármán vortex street [20] cause a neuronal response in the lateral-line system. All previous studies, however, fall short of concretely determining the resulting stimulus at the lateral line. To do so here, we apply to vortex stimuli a method originally proposed by Handelsman and Keller [21], further developed by Geer [22], and introduced into lateral-line research by Hassan [23]. The method introduces a flow potential ϕ_b that models the alteration of the vortex flow due to presence of the fish body. For that purpose the fish body is approximated by a body $\mathcal{B}$ that

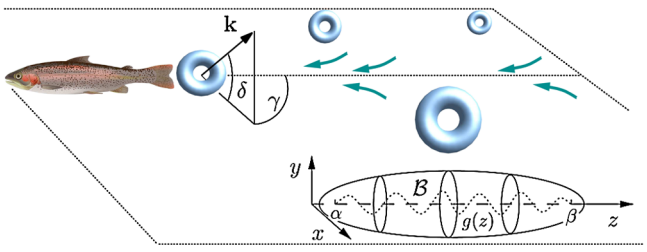

FIG. 1 (color online). A fish's wake consists of vortex rings originating from the tail beats with a velocity component (thick arrows) that compensates for the fish's displacement. Vector **k** describes the orientation of a vortex. A second, rotationally symmetric, fish with body $\mathcal{B}$ is tracking the wake structure. The continuous distribution of hydrodynamic poles $g(z)$ located on the axis of the fish body between α and β (lower picture) ensures that the flow through its surface $\partial\mathcal{B}$ is zero.

is rotationally invariant about the z axis. The potential ϕ_b is then determined in such a way that in combination with the vortex potential ϕ_v it satisfies the boundary condition

$$\frac{\partial}{\partial \mathbf{n}}(\phi_v + \phi_b)|_{\partial\mathcal{B}} = 0,$$

where $\mathbf{n}$ is the normal vector to the fish body. Furthermore, the method is based on the fact that under a Fourier transform with respect to θ in cylindrical coordinates (r, θ) any flow potential ϕ_x can be written [22]

$$\phi_x(\mathbf{r}) = \sum_{n=0}^{\infty} r^n e^{in\theta} \psi_{x,n}(r^2, z), \tag{1}$$

where $x = b$ or v and the ψ_n are functions that depend on r^2 and z only. Formally, the fish body is simply a system of continuous distributions of hydrodynamic poles that are located in the interior of $\mathcal{B}$ in an interval $[\alpha, \beta]$ on the z axis. The flow potential of such a construct is [22]

$$\phi_b(\mathbf{r}) = -\frac{1}{4\pi} \sum_{n=0}^{\infty} \int_{\alpha}^{\beta} \frac{r^n e^{in\theta}(\xi - \alpha)^n(\beta - \xi)^n}{[r^2 + (z - \xi)^2]^{n+1/2}} g_n(\xi) d\xi.$$

Through a direct representation of (1), this sum also constitutes the series of multipole terms of the modeled fish body. The distributions of elementary poles between the boundary points α and β are weighted by a function g_n at each point. Fundamentally, the method of Geer [22] allows the determination of the g_n in such a way that, given ϕ_v, each distribution compensates for the corresponding multipole term of the vortex potential on the fish body surface $\partial\mathcal{B}$. The functional form of g_n thereby depends only on the geometry of $\mathcal{B}$ and the strength of the vortex potential on the axis of the fish body expressed by $\psi_{v,n}(0, z)$ in (1). For an explicit derivation of $g(n)$ and α and β we refer to the original literature [21–23].

It follows that, for the determination of a vortex stimulus as indicated in Fig. 1, it is sufficient to find the vortex potential ϕ_v written in the form of (1). Ring vortices can be described as vortex tubes with strength $\Gamma = \sigma|\omega|$ that is the product of their cross section σ and vorticity $|\omega|$. When a vortex tube becomes thinner and its vorticity increases proportionally, the velocity field around it remains approximately the same. Thus we model a vortex tube by a vortex filament that is the limit of a vortex of zero cross section and infinite vorticity so that its original vortex strength remains constant. To calculate the stationary velocity field of the vortex we can ignore that this sequence of approximations leads to an infinite vortex propagation speed ([12], Sec. 163). To determine the time-dependent velocity field we then simply assume that the vortex propagates with its original speed.

Let the vortex filament enclose the circular area $\mathcal{S}$. Outside a vortex filament, the flow is irrotational so that a flow potential exists. The flow potential of a vortex ring with normal vector $\mathbf{k} = (k_x, k_y, k_z)$ is [[12], Sec. 150]

$$\phi_v(\mathbf{x}) = \frac{\Gamma}{4\pi} \iint_{\mathcal{S}} (k_x \partial_{x'} + k_y \partial_{y'} + k_z \partial_{z'}) \frac{1}{|\mathbf{x} - \mathbf{x}'|} dS'$$

with $|\mathbf{x} - \mathbf{x}'|$ being the Euclidean norm of the vector difference between the integration variable $\mathbf{x}' \in \mathcal{S}$ and the point of observation $\mathbf{x}$. By convention, $\mathbf{k}$ points into the direction of the flow through the vortex. Comparison with a dipole potential $\nabla|\mathbf{x}|^{-1}$ reveals that ϕ_v is equivalent to the potential of a uniform distribution of dipoles lying in $\mathcal{S}$. We therefore use the expansion of the dipole potential Hassan [23] originally derived to determine the lateral-line stimulus originating from oscillating spheres and apply it to vortices (cf. Fig. 1). The origin of the coordinate system lies at the snout of the fish body. The lateral line, say, the trunk one, lies in the x-z plane on the surface of $\mathcal{B}$. The normal vector of the vortex ring $\mathbf{k}$ makes an angle δ with the x-z plane, while the projection of $\mathbf{k}$ in the x-z plane makes an angle γ with the z axis. For $\gamma = \delta = 0$, the normal vector points in positive z direction. The propagation speed of a vortex in a fish's wake is slower than under experimental conditions and even tends to zero [10]. During wake tracking, the intrinsic velocity of the vortex ring is negligible against the swimming speed of the fish. Moreover, $\delta = 0$ because fins usually move in the x-z plane. In our model, vortex rings with relative velocity in the z direction and variable orientation γ therefore correspond to a section of a fish's wake as perceived during wake tracking, whereas for relative motion along the axis of a vortex they are just the vortex rings as used in experiments.

To calculate stimuli we now define p to be the deviation from hydrostatic pressure and use the Bernoulli equation

$$p = \rho \frac{d\phi}{dt} + \frac{1}{2}\rho \mathbf{v}^2 \tag{2}$$

with $\phi = \phi_v + \phi_b$. When a fish glides through the water and passes a vortex laterally, the constant flow due to the motion of the fish as well as the relative motion between vortex and fish have to be taken into account. Typically, the fish moves much faster than the vortex ring, and thus the vortex ring can be considered as resting in space and causing a stationary velocity potential. If a fish passes the vortex ring with swimming speed U in negative z direction, then, in the coordinate system (x, y, z) of the fish, the position of the vortex ring is $z = Z' + Ut$, thus $d\phi(x, y, Z' + Ut)/dt = U\partial\phi/\partial z$, and according to (2)

$$p = \rho U \frac{\partial \phi}{\partial z} + \frac{1}{2}\rho \mathbf{v}^2. \tag{3}$$

Here $\mathbf{v}$ is the total flow of the stationary system and $\partial\phi/\partial z$ covers the relative motion in z direction. If the relative velocity U between vortex and fish is large as compared to $||\mathbf{v}||$, as is the case for a swimming fish, then the pressure distribution is almost solely determined by the first term in (3). The position of a vortex that moves in the direction of its normal vector with $\delta = 0$ is $x = X' + \tilde{U}t \sin\gamma$, $y = Y'$, and $z = Z' + \tilde{U}t \cos\gamma$; thus, for the case of a self-

propagating vortex and a fixed fish,

$$p = \rho\tilde{U}\left(\cos\gamma\frac{\partial\phi}{\partial z} + \sin\gamma\frac{\partial\phi}{\partial x}\right) + \frac{1}{2}\rho\mathbf{v}^2. \quad (4)$$

Experimentally, the core structure of a vortex ring is hardly altered by the physical presence of the fish body from a distance of at least a few (≥ 3) cm onwards [19]. Thus for larger distances circular vortices are the appropriate stimulus to examine. As a real vortex ring propagates, its core radius increases by viscous diffusion, but only so slowly that it retains its structure for over a minute [10]. In nature various vorticities and vortex radii have been observed. Vortex parameters as measured by [13] behind a swimming fish are shown in Table I. The propagation speed $\tilde{U}$ of a vortex results from the ring radii R and R' and the vortex strength Γ ([12], Sec. 163). In computing the stimulus we do neglect viscosity because it only alters the flow field in a so-called boundary layer near the fish's body surface and pressure is constant in any cross section of the boundary layer that is orthogonal to the flow and to the surface ([12], Sec. 371a).

The function $b(z)$ describes the fish body [23]. It is representative as its variation does not significantly change excitation patterns. Furthermore, changes in Y, Z, and δ do not affect the stimulus and are left aside here. Figure 2(c) shows that a change in distance d only scales the amplitude and leaves the shape of the excitation pattern largely unaffected. The same holds true for varying the vortex strength Γ, vortex radius R, and relative velocity U. Thus the lateral-line input does not contain information about Γ, d, R, and U separately, but only through a combination of the four (cf. Table I). A change in vortex ring orientation γ, however, produces very different patterns as discussed below [see Figs. 2(a) and 2(b)].

A vortex stimulus can only be recorded experimentally when the fish is fixed and a vortex passes laterally. Figure 2(d) shows the pressure-difference distributions that we predict for this experimental setup. If the vortex ring propagates relatively slowly, the terms in (4) are of the same order of magnitude, and the pattern exhibits four phases of opposite polarity. Yet the stimulus converges to a two-phasic pattern as $\tilde{U}$ increases.

TABLE I. The parameters of vortex ring and fish body.

Fish body length	BL	20 cm
Distance between pores	Δx	4 mm
Distance between vortex and body	d	0.225 BL
Vortex ring radius	R	0.075 BL
Vortex core radius	R'	0.05 BL
Vortex ring strength	Γ	0.08 BL^2/s
Vortex ring position	X	$d + b(Z)$
	Y	0
	Z	0.5 BL
Vortex ring orientation	δ	0
	γ	$\pi/2$
Swimming speed	U	0.5 BL/s

The experimental setup is described elsewhere [19]. In experiments, a vortex passes a fixed fish laterally and spikes from canal neuromasts are recorded. The radii R and R' of the artificial vortices roughly correspond to those in Table I, except for vortex strength, which is generally lower in experiments. We have therefore used vortex strength Γ and vortex propagation speed U as parameters for a fit of experimental data to theory. Comparing Fig. 2 with Fig. 3, we see that the experimental results of Fig. 3 are, considering the amount of noise in the measurements, consistent with the present theory.

Figures 2(a) and 2(b) show the pressure-difference distributions along the lateral line when fish follow the wake of another fish. Any given vortex orientation results in a specific stimulus each of which consists of two ($\gamma = 0$) or three ($\gamma = \pi/2$) sections of opposite polarity. The transition between these patterns is continuous. In passing we note that stationary oscillating dipoles [2,3,9] and vortex

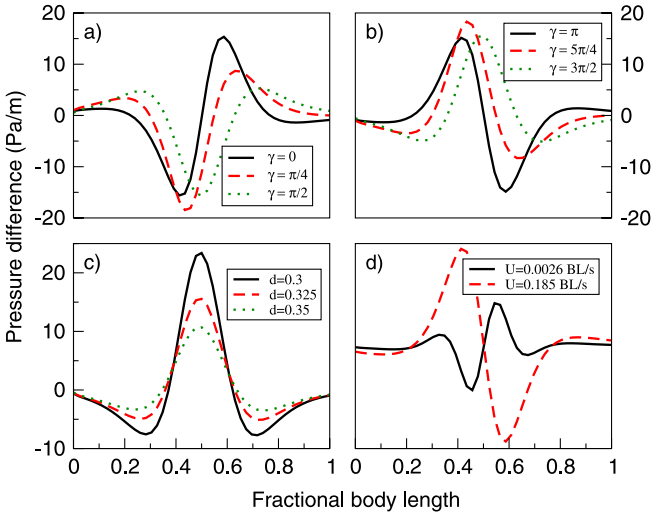

FIG. 2 (color online). Pressure-difference distributions $\partial p/\partial x$ along the (trunk) lateral line due to a vortex ring as a function of position along the body relative to the body length. (a) and (b) During wake tracking vortices with different orientations γ moving in z direction with respect to the fish occur. Any such vortex generates an excitation pattern specific to its orientation angle γ. Patterns corresponding to orientations that differ by $\gamma = \pi/2$ are orthogonal functions so that the orientation of a vortex ring can be determined by projecting the stimulus pattern onto a given basis function. Fish can thus determine the direction they must follow to track their target. (c) Vortices at different distances from the fish generate excitation patterns that only differ in amplitude. The same holds true for changes in Γ, R, and U. (d) For a fixed fish in experiments, a vortex ring with $\gamma \in \{0, \pi\}$ and $\delta = 0$ generates excitation patterns that are either four-phasic or two-phasic depending on the vortex propagation speed $\tilde{U}$. In contrast to cases (a) and (b), there is no one-to-one relation between γ and stimulus. Hence a theory of vortex ring detection cannot be based solely on the experimentally verifiable case (d).

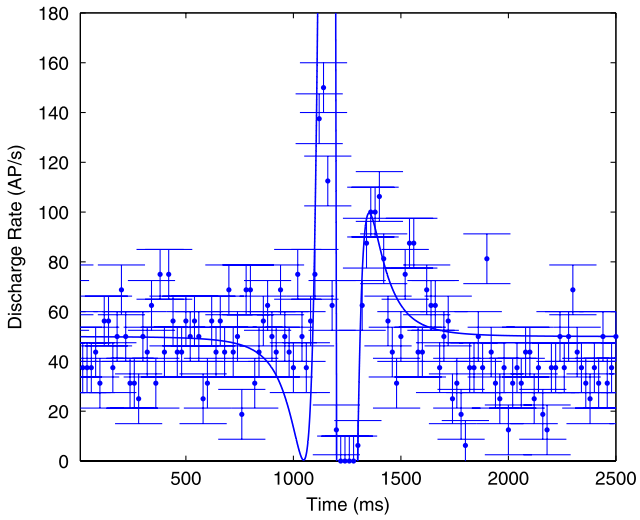

FIG. 3 (color online). Neuronal response ensuing from a canal neuromast (experimental results). The dots represent time-dependent spike rates of a canal neuromast measured when a vortex with $\gamma \in \{0, \pi\}$ and $\delta = 0$ passed a fixed fish, averaged over ten time runs. As the vortex has approximately constant velocity, the recorded time-dependent data match the nervous excitation pattern along the lateral line at one moment of time. Canal neuromasts react to the pressure difference $\Delta p \approx (\partial p/\partial x)\Delta x$ between two adjacent pores shown in Fig. 2. The solid graph is a fit to theory; because of negative hair-cell polarity it is in the present case a mirror image of the black solid line in Fig. 2(d).

wakes described in, e.g., Fig. 2 give rise to the same type of lateral-line stimulus. It is as yet unknown how the nervous system handles this ambiguity.

Because of the spatial congruence of vortex and dipole stimuli their information content can be theoretically treated by means of the same analysis. To this end it has been shown [8] that the stimulus patterns of $\gamma = 0$ and $\gamma = \pi/2$ are orthogonal to one another and that any excitation pattern is a linear combination of the two, allowing a fish to uniquely identify the vortex's orientation by projecting the stimulus in question onto a predetermined excitation pattern. This operation is linear and can be performed by a neuronal network.

Through the mechanisms proposed here the information about the orientation of a vortex ring is accessible to the nervous system. The capability of acquiring this information is of extensive biological significance since the arrangement of vortices in a vortex street characterizes a swimming style.

In short, direct hydrodynamic images are due to instantaneous momentum transfer [5] and wakes to angular-momentum transfer. That is why the latter are of a completely different character than the former. Here we have shown how fish can determine the orientation of a vortex ring through their lateral-line input as the only cue and in this way perform the tracking of wakes, a long-lasting consequence of the conservation of angular momentum in a medium of low viscosity.

The present research has been supported by the European Commission, Future and Emerging Technologies (CILIA), and BCCN—Munich.

[1] S. Coombs, M. Hastings, and J. Finneran, J. Comp. Physiol. A **178**, 359 (1996).
[2] J. Engelmann, W. Hanke, and H. Bleckmann, J. Comp. Physiol. A **188**, 513 (2002).
[3] J.-M. P. Franosch, A. B. Sichert, M. D. Suttner, and J. L. van Hemmen, Biol. Cybern. **93**, 231 (2005).
[4] H. Bleckmann, in *Progress in Sensory Physiology*, edited by O. Ottoson (Springer, New York, 1985), p. 147.
[5] A. B. Sichert, R. Bamler, and J. L. van Hemmen, Phys. Rev. Lett. **102**, 058104 (2009).
[6] S. Coombs and C. Braun, in *Sensory Processing in Aquatic Environments*, edited by S. P. Collin and N. J. Marshall (Springer, New York, 2003), p. 122.
[7] E. J. Denton and J. A. B. Gray, in *Sensory Biology of Aquatic Animals*, edited by J. Atema, R. R. Fay, A. N. Popper, and W. N. Tavolga (Springer, New York, 1988), p. 595.
[8] B. Ćurčić-Blake and S. M. van Netten, J. Exp. Biol. **209**, 1548 (2006).
[9] J. Goulet, J. Engelmann, B. P. Chagnaud, J.-M. P. Franosch, M. D. Suttner, and J. L. van Hemmen, J. Comp. Physiol. A **194**, 1 (2008).
[10] W. Hanke, C. Brücker, and H. Bleckmann, J. Exp. Biol. **203**, 1193 (2000).
[11] J. Gray, J. Exp. Biol. **10**, 391 (1933).
[12] H. Lamb, *Hydrodynamics* (Cambridge University Press, Cambridge, England, 1932), 6th ed.
[13] E. Drucker and G. Lauder, Integr. Comp. Biol. **42**, 243 (2002).
[14] W. Hanke and H. Bleckmann, J. Exp. Biol. **207**, 1585 (2004).
[15] K. Pohlmann, F. W. Grasso, and T. Breithaupt, Proc. Natl. Acad. Sci. U.S.A. **98**, 7371 (2001).
[16] A. J. Kalmijn, in *Sensory Biology of Aquatic Animals*, edited by J. Atema, R. R. Fay, A. N. Popper, and W. N. Tavolga (Springer, New York, 1988), p. 83.
[17] S. M. van Netten, Biol. Cybern. **94**, 67 (2006).
[18] J. Lighthill, Phil. Trans. R. Soc. B **341**, 129 (1993).
[19] B. P. Chagnaud, H. Bleckmann, and J. Engelmann, J. Exp. Biol. **209**, 327 (2006).
[20] B. P. Chagnaud, H. Bleckmann, and M. H. Hofmann, J. Comp. Physiol. A **193**, 753 (2007).
[21] R. Handelsman and J. Keller, J. Fluid Mech. **28**, 131 (1967).
[22] J. Geer, J. Fluid Mech. **67**, 817 (1975).
[23] El-S. Hassan, Biol. Cybern. **69**, 525 (1993).